Journal of Alloys and Compounds 509 (2011) 4242–4246

Contents lists available at ScienceDirect

Journal of Alloys and Compounds

journal homepage: www.elsevier.com/locate/jallcom

Effect of high undercooling on Co–Ni–Ga ferromagnetic shape memory alloys

Junzheng Li, Jianguo Li*

School of Materials Science and Engineering, Shanghai Jiao Tong University, Shanghai 200240, PR China

ARTICLE INFO

Article history:
Received 12 November 2010
Received in revised form
14 December 2010
Accepted 15 December 2010
Available online 23 December 2010

Keywords:
Sub-grain
Undercooling
Co–Ni–Ga
Ferromagnetic shape memory alloy

ABSTRACT

$Co_{45}Ni_{25}Ga_{30}$ ferromagnetic shape memory alloys were treated by glass fluxing combined with superheating cycling. The effect of high undercooling on solidified microstructure and transformation temperatures was investigated. The martensite lath is obviously refined and a mass of sub-grains are produced with the increase of undercooling. Undercooling rapid solidification introduces a number of dislocations and large internal stress, which give rise to the production of sub-grains in recovery. During the following annealing process, these sub-grains can gradually recrystallize and grow up with an amount of γ' phase precipitated. Meanwhile, transformation temperatures of undercooled alloys are greatly elevated compared with those of as cast, which results from the large internal stress, and gradually reduce with the heating time.

1. Introduction

As a new ferromagnetic shape memory alloy (FSMA), Co–Ni–Ga has recently attracted a great deal of attention owing to its magnetic-controlled two-way shape memory effect [1], high martensitic transformation temperatures [2] and high ductility [3]. Sato et al. reported that the Co–Ni–Ga textured ribbons prepared by the melt-spinning rapid solidification exhibited large magnetic-field-induced strain (MFIS) [4]. The dimensions of these melt-spun ribbons, however, are usually very small and hence seriously restrict their applications. As has been demonstrated, if an alloy melt reaches a certain undercooling (ΔT), the rapidly solidified microstructure tends to possess refined and textured grains, such as in Ni–Cu alloys [5,6], super-alloys (DD3 alloys) [7,8] and Fe–Ga alloys [9,10]. Thus, it is expected to obtain bulk Co–Ni–Ga textured alloys with improved properties by undercooling rapid solidification.

Interestingly, Dragnevski et al. [11] discovered in the undercooled pure Cu sample a high density of subgrains, which were deemed to result from some redistribution of line defects introduced by rapid solidification. A similar phenomenon was found in undercooled DD3 single crystal super-alloys [8]. These results suggest that high undercooling can introduce large internal stress and in turn induce fine sub-grains, which will inevitably affect material properties. As is known, sub-grains are usually introduced in metal materials by thermo-mechanical processing and there are a lot of relative researches [12–15]. However, there are few studies concerning sub-grains introduced in FSMAs, and no particular discussions on the relationship between sub-grains and undercooling were reported, let alone those about the effect of sub-grains on transformation temperatures. In this paper, $Co_{45}Ni_{25}Ga_{30}$ alloys were treated by glass fluxing combined with superheating cycling and following annealing. The effect of undercooling on the microstructure, especially the production of sub-grains, and the transformation temperatures were investigated.

2. Experimental

Ingots of $Co_{45}Ni_{25}Ga_{30}$ alloys were prepared by arc-melting under an argon atmosphere. They were melted four times and homogenized in a vacuum heat treatment furnace at 1000 °C for 48 h in order to achieve composition homogenization. Samples with the mass in 1.5 g were cut from the ingots for the undercooling experiments which were performed in a high frequency induction unit. Glass fluxing combined with superheating cycling was used to achieve a reasonable large undercooling. The fluxed glass, consisting of 70 wt.% $Na_2B_4O_7$, 30 wt.% NaSiCa, was employed as the denucleating agent. The undercooling experimental apparatus and experimental process were described in our previous report [16]. Some undercooled samples underwent annealing at 800 °C for 1 h, followed by furnace cooling.

The optical microscopy (Neo-plot1 OM), the scanning electron microscopy (SEM520 SEM) and the transmission electron microscopy (JEM-2100 TEM) were used to examine the microstructure. Chemical composition determination was carried out using energy dispersion X-ray spectroscopy (EDS). The transformation temperatures were determined by differential scanning calorimeter (Perkin-Elmer DSC) with the testing temperature scope from −50 °C to 300 °C and the heating-cooling rate of 10 °C/min. Transmission electron microscopy (TEM, JEM-2100) examination was carried out on a thin foil. The thin foils for TEM were electrochemically polished by the twin jet method in a solution of 20% HNO_3 and residual ethanol.

* Corresponding author. Tel.: +86 21 54744119; fax: +86 21 54744119.
E-mail address: lijg@sjtu.edu.cn (J. Li).

0925-8388/$ – see front matter © 2010 Elsevier B.V. All rights reserved.
doi:10.1016/j.jallcom.2010.12.120

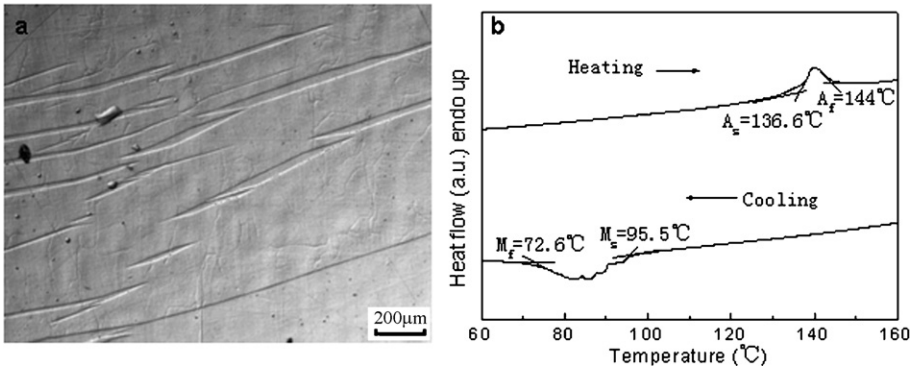

Fig. 1. Optical image (a) and DSC curves (b) of as-cast $Co_{45}Ni_{25}Ga_{30}$ alloys.

3. Results and discussion

A typical single martensite morphology is observed in as-cast $Co_{45}Ni_{25}Ga_{30}$ alloys, as shown in Fig. 1a. The martensite lath is as coarse as a few hundred microns in width. Martensitic transformation takes place during the solidification process, indicating that the martensitic transformation start temperature (M_s) is higher than room temperature. As the DSC curves show in Fig. 1b, the M_s, the martensitic transformation finish temperature (M_f), the austenitic transformation start temperature (A_s) and the austenitic transformation finish temperature (A_f) are respectively 95.5 °C, 72.6 °C, 136.6 °C and 144.0 °C, which testify that $Co_{45}Ni_{25}Ga_{30}$ alloys are martensite state at room temperature and have high transformation temperatures indeed.

A maximum undercooling for $Co_{45}Ni_{25}Ga_{30}$ alloys reaches 220 °C. The EDS analysis of rapidly solidified samples with different undercoolings confirms that no chemical reaction occurred between the alloy melt and the denucleating glass. Accordingly, the alloy composition remains almost unchanged by undercooling (Table 1). The microstructure of $Co_{45}Ni_{25}Ga_{30}$ alloys with a wide range of undercooling from 66 °C to 220 °C is shown in Fig. 2. It can be seen that the samples at various undercoolings possess single martensite phase, but the morphologies of martensite change observably with the undercooling increasing. When the undercooling is about 66 °C, two oriented types of martensite variant intersect in the sample at an angle of about 30° with the martensite lath width of about 75 μm (Fig. 2a). However, only one variant remains and the other disappears when the undercooling rises to 100 °C (Fig. 2b), and the martensite lath becomes smooth and straight with the undercooling increasing (Fig. 2b–d). Meanwhile, the martensite lath width dramatically declines with the undercooling increasing, as is shown in Fig. 3. It decreases from 75 μm at undercooling of 66 °C to no more than 20 μm at undercooling of 220 °C, which illuminates that the lath can be remarkably refined by undercooling.

Table 1
Chemical composition of $Co_{45}Ni_{25}Ga_{30}$ alloys measured by EDS.

Alloy	Chemical composition (at.%) (±0.05%)		
	Co	Ni	Ga
As-cast	44.73	25.19	30.07
ΔT=220 °C	45.55	25.39	29.06

Since the martensite transformation is the process of martensite nucleation and growth, the refinement of martensite lath with

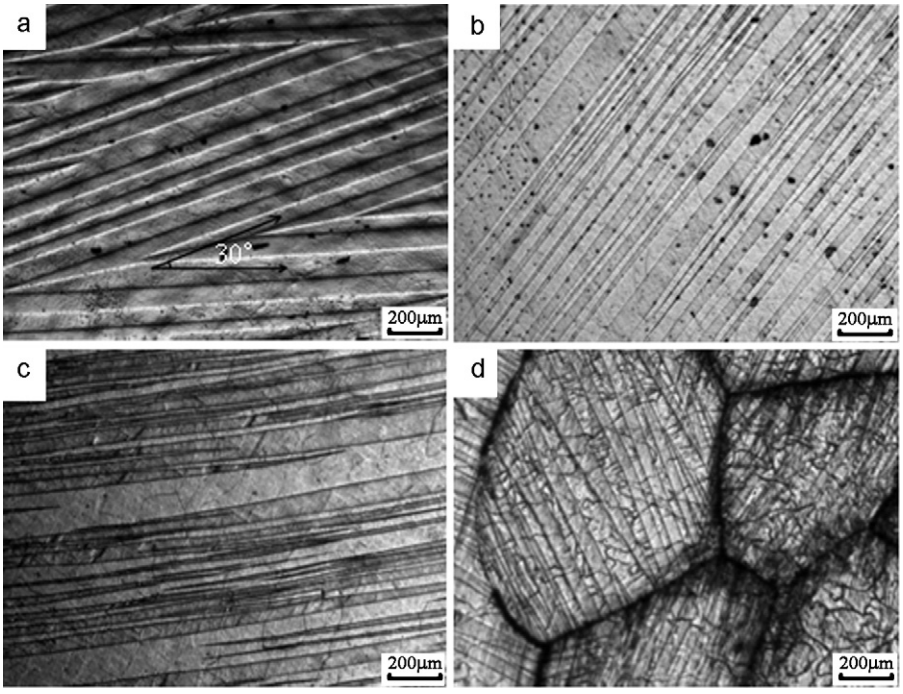

Fig. 2. Microstructure of $Co_{45}Ni_{25}Ga_{30}$ alloys with undercooling of (a) 66 °C, (b) 100 °C, (c) 186 °C, (d) 220 °C.

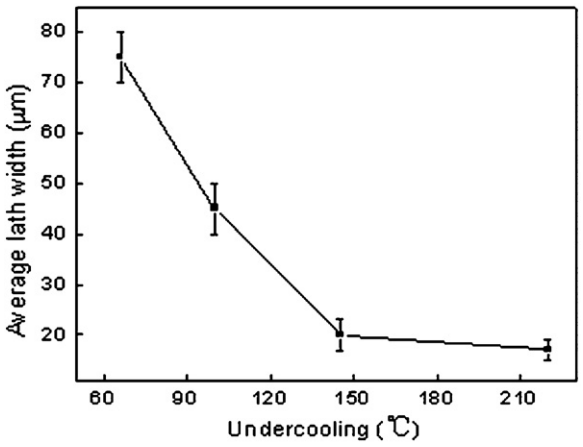

Fig. 3. Martensite lath width as a function of the undercooling of $Co_{45}Ni_{25}Ga_{30}$ alloys.

undercooling can be explained by the classical nucleation theory [17]. The steady state nucleation rate, I, can be expressed as [17]

$$I = \frac{k_B T \xi N_A}{3\eta(T) a_0{}^3} \exp\left(-\frac{\Delta G * f(\theta)}{k_B T}\right) \quad (1)$$

where K_B is the Boltzmann constant, ξ the potential nucleation sites fraction, N_A the Avogadro's number, a_0 the interatomic distance, T the system temperature, and $\eta(T)$ the temperature-dependent viscosity of the undercooled melt. The temperature-dependent viscosity can be approximated by the Vogel–Fulcher–Tammann equation

$$\eta(T) = \eta_0 \exp\left(\frac{A}{T - T_0}\right) \quad (2)$$

where η_0 is the viscosity of alloy in melting temperature and T_0 the ideal glass transition temperature ($\approx 2/3T_m$). The activation energy ΔG^* for the formation of a critical nucleus is given by

$$\Delta G^* = \frac{16\pi\sigma^3}{3\Delta G_V{}^2} f(\theta) \quad (3)$$

where σ is the interfacial energy of the solid–liquid interface, $f(\theta)$ the catalytic potency factor for heterogeneous nucleation, and ΔG_V the Gibbs free energy difference for phase formation. ΔG_V is calculated by [18]

$$\Delta G_V = \Delta S_f \Delta T - \frac{\Delta S_f}{Ln(T_L/T_0)}\left[\Delta T - TLn\left(\frac{T_L}{T}\right)\right] \quad (4)$$

where ΔS_f is the entropy of fusion, and T_L the liquidus temperature.

Based on Eqs. (1)–(4) above, the nucleation rate grows with increasing undercooling and causes decreasing width of the martensitic lath in $Co_{45}Ni_{25}Ga_{30}$ alloys.

What should be noted is that a well-developed network of both high angle of boundaries and low angle of sub-boundaries can be seen at the undercooling of 220 °C, (Fig. 2d). The microstructure exhibits coarse equiaxed grain with the size of 400 μm and the boundaries are clear. However, it is difficult to distinguish boundaries in the alloys with small undercoolings (Fig. 2a–c), not to mention in the as-cast alloy (Fig. 1a). More importantly, a mass of fine sub-grains with 50 μm in size are introduced in these coarse equiaxed grains (Fig. 2d), which are seldom found in normal solidification process except in that of undercooled DD3 super-alloys and pure Cu samples [8,11]. Meanwhile, there is only one type of variant in one grain; the variant can traverse the sub-boundaries but stops at the boundaries, which may be attributed to the fact that the sub-boundaries are low-energy configurations but the boundaries are high-energy ones.

As is mentioned in the literature [12–15], sub-grains usually appear in high deformation metal materials. Studies on thermo-mechanical processing have proved that deformation structures store high internal stress and release the stored energy by recovery, recrystallization and eventual grain growth during the following annealing [12,13]. These 'softening' processes involve a set of micromechanisms for the motion and annihilation of point defects, dislocations and boundaries [14,15]. That fine sub-grains are induced in undercooled Co–Ni–Ga alloys by undercooling rapid solidification is similar to what happened to the thermo-mechanical processing. Fig. 4 shows the schematics of the micromechanism of the sub-grain formation during recovery. According to the recovery micromechanism on thermo-mechanical processing, free and random dislocations organize into dislocation walls or sub-boundaries and result into polygonization [19,20]. At the rapid solidification stage after recalescence, the sudden volume contraction and the cavity collapse of undercooled liquid would result in a large number of vacancies, interstitials and dislocations [21], which increase with the undercooling and generate an internal stress field [22]. These dislocations introduced by undercooling rapid solidification are abundant and random (Fig. 4a); the internal stress gradually increases with the sample cooling down and induces recovery. Some closely spaced dislocations of opposite sign climb and/or cross slip to annihilate (Fig. 4b and c), then the remainder rearranges into net sub-boundaries (Fig. 4d). Meanwhile, these point defects (vacancies and interstitials) can be annihilated by diffusion of dislocations.

To further investigate the possible rearrangement of dislocations, TEM analysis and higher magnification of optical micrograph were carried out on the undercooled alloys of 66 °C and 220 °C (Fig. 5). From the TEM image of the sample undercooled by 66 °C, as is shown in Fig. 5a, it is evident that the dislocations in the martensite lath have realigned into walls, which stuck together to form a fine array of sub-boundaries. The optical micrograph also demonstrates that a large number of sub-grains have already been induced at lower undercooling of only 66 °C (Fig. 5b). For the undercooling of 220 °C, these sub-grains take more distinct sub-boundaries compared with those of 66 °C (Fig. 5c), which also indicates larger internal stress of 220 °C and would lead to more reduction of internal energy. These sub-grains would recrystallize and grow up while the large internal stress is completely released during the following annealing. Fig. 6 shows the microstructure of $Co_{45}Ni_{25}Ga_{30}$ alloys undercooled by 220 °C annealed at 800 °C for 1 h. It is found that sub-grains have obviously grown up and the average grain size is

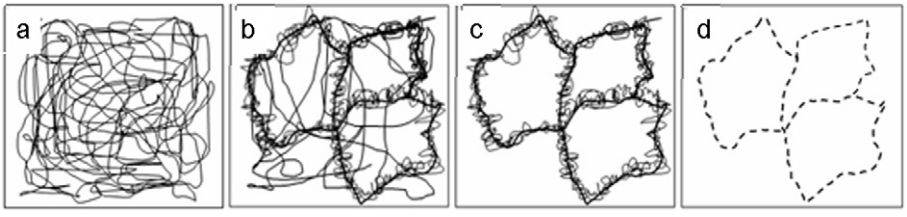

Fig. 4. Schematics of random dislocation tangles through cell structures to sub-grains during recovery.

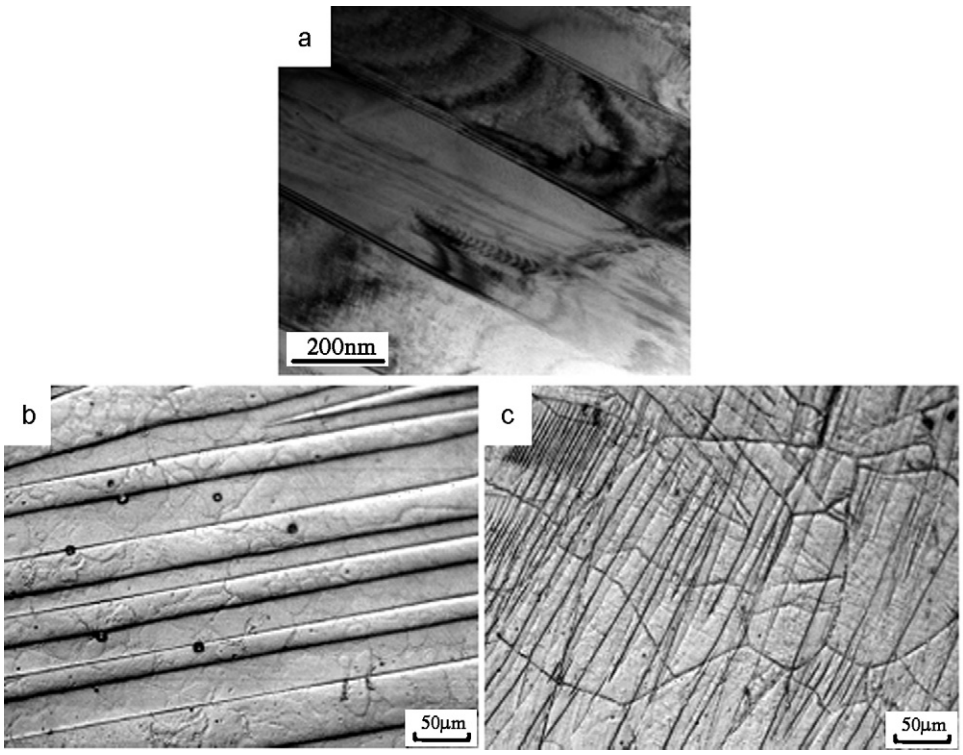

Fig. 5. TEM image of several dislocation walls of $Co_{45}Ni_{25}Ga_{30}$ alloys undercooled by 66 °C (a), microstructures at higher magnification of the alloy undercooled by 66 °C (b), 220 °C (c).

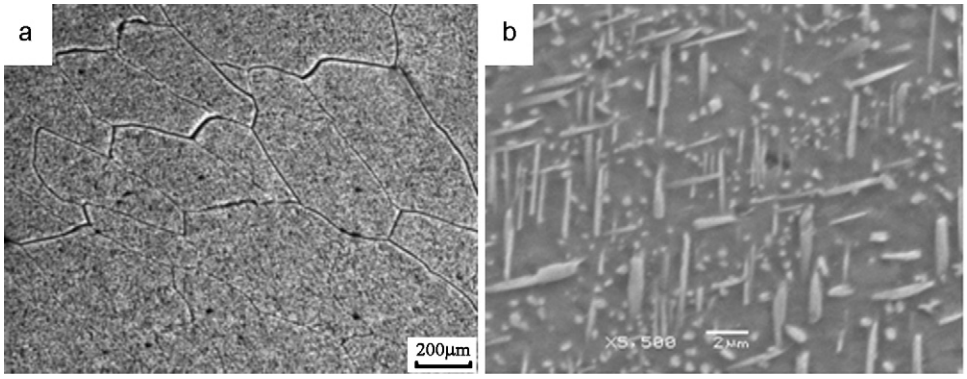

Fig. 6. Microstructure of the $Co_{45}Ni_{25}Ga_{30}$ alloy with undercooling of 220 °C annealed at 800 °C for 1 h (a), SEM with higher magnification of an amount of precipitate (b).

more than 200 μm. Meanwhile, it can be seen that these grains own near quadrate morphology and have a uniform growth direction (Fig. 6a), which might demonstrate that the large internal stress introduced by undercooling rapid solidification has an oriented direction and induces these sub-grains growing in a given direction. The SEM image shows an amount of fine precipitate dispersing uniformly in the matrix (Fig. 6b), whose morphology exhibits a needle-like or particle structure. And this kind of precipitation was considered as low-temperature equilibrium ordered γ' phase [23].

Table 2 shows the transformation temperatures of $Co_{45}Ni_{25}Ga_{30}$ alloys. The transformation temperatures (M_s, M_f, A_s, A_f) of the alloy undercooled by 220 °C respectively reach 143.0 °C, 119.5 °C, 180.0 °C and 192.5 °C, which are all almost 50 °C higher than those of as-cast alloys. It confirms that the high undercooling evidently raises the transformation temperatures. Following the mechanism of elastic strain energy [24], when the martensite lath was plastically deformed in the highly undercooled sample, the variant self-accommodation effect was damaged and the elastic strain energy stored in variants was released by residual internal stress, thus the chemical energy drove the reverse transformation temperatures to increase. On the contrary, the internal stress assisted the austenite to transform into martensite during the cooling process, which would result in the increase of martensite transformation temperatures. In order to further investigate the effect of internal stress on the transformation temperatures, the DSC test with three cycles at a wide temperature scope was carried. The influence of testing cycle time on transformation temperatures of $Co_{45}Ni_{25}Ga_{30}$ alloys undercooled by 220 °C is shown in Fig. 7. One can find that transformation temperatures, especially the reverse transformation temperatures, have obvious changes within the three cycles

Table 2
Transformation temperature of $Co_{45}Ni_{25}Ga_{30}$ alloys measured by DSC.

Alloy	Transformation temperature (°C) (±0.5)			
	M_s	M_f	A_s	A_f
As-cast	95.5	72.6	136.6	144.0
ΔT = 220 °C	143.0	119.5	180.0	192.5

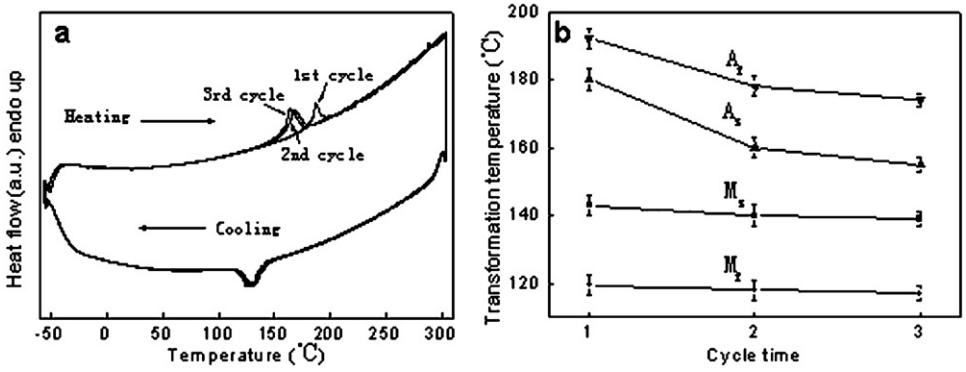

Fig. 7. DSC curves of $Co_{45}Ni_{25}Ga_{30}$ alloys undercooled by 220 K (a), influence of cycle time on the transformation temperatures (b).

(Fig. 7a). The exact change of transformation temperatures with the cycle time is shown in Fig. 7b. It can be seen that the reverse transformation temperatures decrease over 20 °C during the cycles, while the changes of martensite transformation temperatures are very little. The DSC test is conducted from −50 °C to 300 °C, the process of which is equal to the heat treatment of the sample. The undercooled sample is gradually heated up to 300 °C, the internal stress would be partly released, and the residual internal stress becomes less and less with the testing time. As a result, transformation temperatures of the undercooled alloy, especially the reserve transformation temperatures, decrease gradually with the cycle time. A similar result was found in undercooled $Co_{46}Ni_{27}Ga_{27}$ alloys [25], which implied that the A_s temperature increases with the undercooling, i.e. a higher undercooling induces larger internal stress and thus leads to a higher A_s. It can be seen that the effect of high undercooling on the transformation temperatures is considerable.

4. Conclusion

The effect of undercooling on microstructure evolution and transformation temperatures of $Co_{45}Ni_{25}Ga_{30}$ martensite alloys is significant. When the undercooling is 66 °C, there are two types of martensite variants which intersect at 30° in the sample. With the increase of undercooling, the martensite lath is obviously refined and a mass of sub-grains are induced. A number of dislocations and large internal stress give rise to the occurrence of sub-grains during the recovery process. The sub-grains recrystallize and grow into coarse grains during the annealing process. Meanwhile, the transformation temperatures of undercooled alloys are significantly raised by high undercooling and gradually decrease with the heating time.

Acknowledgements

The authors express their appreciation for the financial support of the National Natural Science Foundation (No. 50671068).

References

[1] Y.X. Li, H.Y. Liu, F.B. Meng, L.Q. Yan, G.D. Liu, X.F. Dai, M. Zhang, Z.H. Liu, J.L. Chen, G.H. Wu, Appl. Phys. Lett. 84 (2004) 3594.
[2] J. Liu, H.X. Zheng, M.X. Xia, Y.L. Huang, J.G. Li, Scripta Mater. 52 (2005) 935.
[3] K. Oikawa, T. Ota, F. Gejima, T. Ohmori, R. Kainuma, K. Ishida, Mater. Trans. 42 (2001) 2472.
[4] M. Sato, T. Okazaki, Y. Furuya, M. Wuttig, Mater. Trans. 44 (2003) 372.
[5] Z. Zhou, H. Fu, J. Mater. Sci. Lett. 19 (2000) 1491.
[6] G. Song, M. Lee, W. Kim, D. Kim, Z. Zhang, X. Lin, G. Yang, Y. Zhou, Mater. Trans. 41 (2000) 1569.
[7] F. Liu, X.F. Guo, G.C. Yang, J. Cryst. Growth 219 (2000) 489.
[8] F. Liu, G.C. Yang, X.F. Guo, Mater. Sci. Eng. A 311 (2001) 54.
[9] W.Z. Ma, H.X. Zheng, M.X. Xia, J.G. Li, J. Alloys Compd. 379 (2004) 188.
[10] J.K. Zhou, J.G. Li, J. Alloys Compd. 461 (2008) 113.
[11] K.I. Dragnevski, R.F. Cochrane, A.M. Mullis, Mater. Sci. Eng. A 375–377 (2004) 479.
[12] S. Straub, W. Blum, H.J. Maier, T. Ungár, A. Borbély, H. Renner, Acta Mater. 44 (1996) 4337.
[13] B. Kockar, I. Karaman, J.I. Kim, Y.I. Chumlyakov, J. Sharp, C.J. Yu, Acta Mater. 56 (2008) 3630.
[14] W. Blum, Y.J. Li, K. Durst, Acta Mater. 57 (2009) 5207.
[15] Y. Huang, F.J. Humphreys, Acta Mater. 45 (1997) 4491.
[16] J.Z. Li, J. Liu, M.X. Zhang, J.G. Li, J. Alloys Compd. 499 (2010) 39.
[17] D. Turnbull, Contemp. Phys. 10 (1969) 473.
[18] D.M. Herlach, F. Gillessen, T. Volkmann, M. Wollgarten, K. Urban, Phys. Rev. B 46 (1992) 5203.
[19] R.W. Cahn, J. Inst. Met. 76 (1949) 121.
[20] D. Kuhlmann-Wilsdorf, Mater. Sci. Eng. A 113 (1989) 1.
[21] J.D. Hunt, K.A. Jackson, J. Appl. Phys. 37 (1966) 254.
[22] G.L. Powell, L.M. Hogan, Trans. Metall. Soc. AIME 245 (1969) 407.
[23] J. Liu, H. Xie, Y.Q. Huo, H.X. Zheng, J.G. Li, J. Alloys Compd. 420 (2006) 145.
[24] M. Piao, K. Otsuka, S. Miyazaki, H. Horikawa, Mater. Trans. 10 (1993) 919.
[25] J. Liu, Y.Q. Huo, H.X. Zheng, J.G. Li, Mater. Lett. 60 (2006) 1693.